FINITE ELEMENT MODELLING OF MOISTURE UPTAKE IN CARBON FIBRE / EPOXY COMPOSITES: A MULTI-SCALE APPROACH

S. Alston[1*], F Korkees[1], C. Arnold[1]

[1]*Materials Research Centre, Swansea University, Singleton Park, Swansea SA2 8PP, UK*
**s.alston@swansea.ac.uk*

Keywords: modelling carbon epoxy moisture.

Abstract
Overall diffusivities for a non-homogeneous, anisotropic composite structure were predicted by finite element modelling of steady state diffusion through a semi-infinite plate perpendicular to the diffusion direction. This forms the basis of a multi-scale modelling approach, which allows the results of simulation at the microstructural level to be used to predict the diffusivities for a range of composite types. Data from water uptake trials of unidirectional composite samples were used to derive diffusivities orthogonal to the fibres both within and through layers, and comparison of these with predicted values showed good agreement. The predicted diffusivities were very dependent on accurate representation of the detailed microstructure.

1 Introduction

The increasing use of carbon fibre / epoxy composites for large scale manufacturing, particularly in the aerospace sector, has led to greater interest in the effect of the operating environment on these materials. In particular, the absorption of water into the epoxy resin affects the mechanical properties of the composite and must be allowed for in the design of structures. The assumption of the worst case "hot-wet" condition leads to the use of additional material and hence weight and fuel use, when in fact the interior of larger components may never reach this state. The detailed modelling of water uptake can enable more tailored design.

The ultimate aim of modelling large scale components can be achieved by using a multi-scale approach, starting from the behaviour at the level of individual fibres. At each scale the properties of a representative unit cell can be derived, then incorporated into larger scale models using a more continuum-based approach. In general the complexity of structures leads to the need for finite element (FE) modelling to predict unit cell behaviour. This work looks specifically at microstructural-scale modelling and validation of the behaviour of a uni-directional (UD) composite in a range of humidity and temperature conditions. In general this will have different diffusivity in the three directions i.e. along the fibres (x), across the fibres within a layer (y), and through the layers (z). A number of studies have looked at the derivation of these three values from measured water uptake data which is normally a result of diffusion from all sides. Methods include thin samples with diffusion mainly in one direction

[1], samples of varying sizes with correction for edge effects [2, 3], and protection of some sides using foil [4]. Diffusivity through the layers has been found to be a factor of anywhere between four [2] and twenty [4] times less than that along the fibres.

The predicted diffusivity of a unit cell at the level of individual fibres has been found to depend significantly on the fibre volume fraction and arrangement, which affect both the gap size between fibres and the path length of diffusion through the matrix. Choi [1] proposed that the diffusivity was proportional to $(1/\text{path length})^2$. Modelling using a regular fibre arrangement predicts a significantly higher diffusivity than a random fibre distribution which tends to lead to smaller gaps and longer diffusion paths [5], and the random distribution has been found to give results closer to measured data [6, 7]. Model validation can be carried out using various methods. These include comparison of the predicted and measured water uptake curves for the composite following modelling at a number of scales [8, 7], the ability to consistently estimate resin diffusivity using FE modelling and/or statistical fitting [6, 3], and comparison of predicted and measured diffusivity in the z-direction [7].

This work aimed to model and validate a detailed UD composite structure. Experimental values of diffusivity in the y- and z- directions were derived from measured data using thin samples corrected for edge effects. These were compared with predictions from FE modelling at two scales based on the detailed microstructure.

2 Experimental derivation of composite diffusivity

2.1. Materials

Samples of unfilled epoxy resin were supplied from the manufacturer with dimensions 33 x 19.9 x 4 mm. Carbon fibre / epoxy composite using the same epoxy resin was supplied by Airbus Operations Ltd as a UD sheet approximately 25 mm thick. Three orientations of thin samples were cut from this, such that for orientations 1, 2 and 3 diffusion was primarily in the x-, y- and z-direction respectively. For each orientation, samples were cut with thicknesses 1 mm, 2 mm and 4 mm in the main diffusion direction, with the other two dimensions approximately 25 mm. Optical microscopy was used to identify the composite structure, as shown in figure 1.

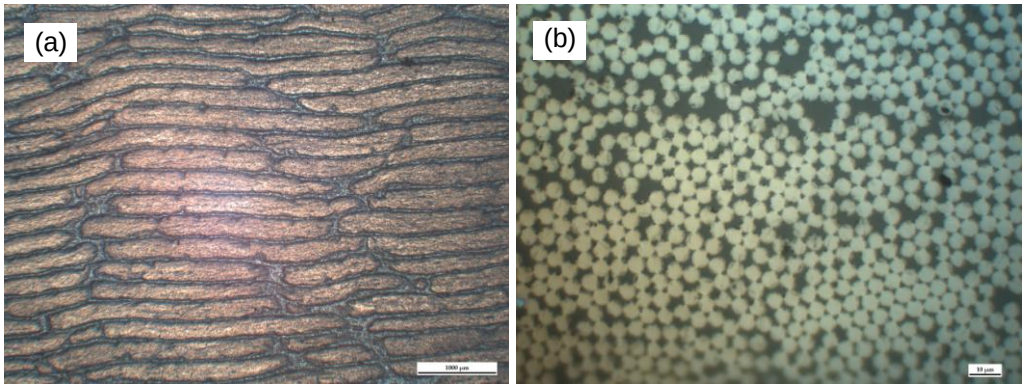

Figure 1. Cross section of UD composite (a) 20x magnification showing fibre-rich regions separated by resin layers, and (b) 800x magnification of a fibre-rich region

Typically the fibre-rich regions were found to be around 225 μm thick, and the resin layers between them approximately 10% of that. The average fibre diameter was 6 μm. Fibre

volume fraction (V_f) was measured by counting the number of fibres in three representative fibre-rich areas and calculating the corresponding area (and hence volume) fraction. This gave $V_f = 0.75$ for the fibre-rich region.

2.2. Water uptake measurements

Samples as described above were dried at 70°C with dessicant until no further weight loss was observed. Two of each type were then conditioned over long periods at each of the following conditions:

23°C immersed in water; 40°C immersed in water; 70°C immersed in water;
70°C at 45% relative humidity (RH); 70°C at 60% RH; 70°C at 85% RH.

Weight measurements were taken at regular but decreasing intervals using a balance with a resolution of 0.01mg. All surface water was removed from the sample prior to weighing. The percentage weight increase was plotted against √(time) with the expectation that the samples would show Fickian behaviour and so the first part of this graph would be linear.

2.3. Derivation of diffusion coefficients

Although each orientation of the composite samples corresponded to diffusion mainly in one of the three material directions, edge effects meant that all samples would see diffusion to some extent in all three directions. This was compensated for using the factor proposed by Starink, Starink and Chambers [3]. For example, for a sample with its main diffusion in the x direction and thickness h in that direction, which is smaller than its width W and length L, the water uptake can be treated as Fickian diffusion with an apparent diffusivity D_{app} given by equation (1), and related to the gradient g_{meas} and saturation weight percent m_∞ of the water uptake graph by equation (2).

$$D_{app} = D_x \left(1 + 0.54 \frac{h}{W} \sqrt{\frac{D_y}{D_x}} + 0.54 \frac{h}{L} \sqrt{\frac{D_z}{D_x}} + 0.33 \frac{h^2}{WL} \sqrt{\frac{D_y D_z}{D_x^2}} \right)^2 \quad (1)$$

$$\frac{g_{meas}}{m_\infty} = \left(\frac{4}{h}\right) \sqrt{\frac{D_{app}}{\pi}} \quad (2)$$

Similar equations apply to samples with their main diffusion in the y- or z- directions. The water uptake for all samples therefore depends on all of D_x, D_y and D_z. For diffusion in the composite along the fibres, since the diffusion path is the same as in the neat resin, the value of D_x would be expected to be the same as D_r. An optimisation method was used to derive values of D_y and D_z which most accurately predicted g_{meas} for all samples at a particular condition.

2.4. Results

Figure 2 shows a typical water uptake graph. It was found that even after 3 years the weight was continuing to rise gradually. This behaviour has been observed elsewhere and is discussed in a separate paper [9]. Since the FE model described here dealt specifically with Fickian diffusion it was necessary to extract the Fickian component of the curve. The long

term behaviour appeared to be linear with √(time) and it was assumed that this applied throughout the conditioning. The gradient of a tangent to the later part of the curve was therefore used to remove the long term effect and leave an estimate of the Fickian graph. This was used to estimate m_∞ and then D_y and D_z as described above. In the case of the unfilled epoxy, a single diffusivity D_r was derived. The results are shown in table 1. Typically D_z was between 5 and 7 times smaller than D_x, within the range found in other studies [1, 2, 4].

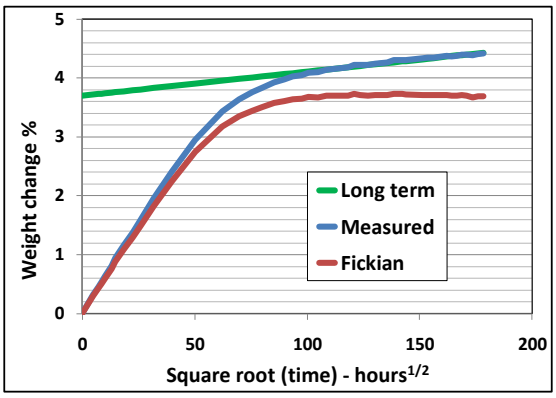

Figure 2. Extraction of Fickian behaviour from long term water uptake measurements

	Saturation, weight % m_∞		Diffusivity, m^2/sec x 10^{14}		
Condition	Epoxy	Composite	$D_x=D_r$	D_y	D_z
23°C in water	3.7	1.36	12.1	4.8	2.3
40°C in water	3.8	1.35	32.0	13.1	5.0
70°C in water	3.95	1.34	141	71.9	22.6
70°C, 45% RH	0.7	0.35	186	91.9	32.6
70°C, 60% RH	1.1	0.6	185	70.8	25.8
70°C, 85% RH	2.4	1.08	159	70.8	24.2

Table 1. Saturation values and diffusivities derived from measured data

3 Prediction of composite diffusivity using multi-scale modelling

3.1. Multi-scale representation of composite samples

Given the composite structure described above, modelling of these samples was carried out at two scales. Initially, a number of unit cells were constructed with individual parallel UD carbon fibres within an epoxy matrix, with the fibre layout and volume fraction matching typical areas of the fibre-rich regions as shown in figure 1(b). It was assumed that no moisture was absorbed by the fibres, so that all diffusion was through the epoxy resin. As expected, D_x was calculated to be the same as D_r. Since there was no visual difference between the y- and z- directions in the fibre-rich regions, an average value D_{yz} was predicted from a number of fibre arrangements. The saturation moisture content M_∞ (kg/m^3) for the structure followed from the fibre volume fraction according to equation (3).

$$M_\infty = (1-V_f)M_{\infty,epoxy} + V_f M_{\infty,fibre/yarn} \quad (3)$$

A larger scale structure was then created consisting of a representative area of yarns in an epoxy matrix as shown in figure 1(a), where the yarns had the properties of the fibre-rich regions just calculated. The yarns were parallel in the x-direction, so that again $D_x = D_r$, and

values of D_y and D_z were predicted. These were compared with the experimental D_y and D_z values in section 2.4.

3.2. Diffusion equation

The basic diffusion model is given by Fick's second law which is traditionally written in terms of the three-dimensional diffusion tensor [D] (m^2/sec) and moisture concentration field C (kg/m^3). This formulation however introduces some complexity at material boundaries, such as those between yarns and resin, where the concentration is discontinuous. At these boundaries the relative concentration $C^* = C/M_\infty$ is continuous. The equation was therefore implemented in the form

$$\nabla^T [P] \nabla C^* - \frac{\partial}{\partial t} C^* = 0 \tag{4}$$

where [P] is the three dimensional permeability tensor = M_∞ [D] (kg/m/sec) [5, 7]. The finite element representation of this was solved using a pre-conditioned conjugate gradient method.

3.3. Boundary conditions

To obtain values of the diffusivities D_x, D_y and D_z for a unit cell, if Fickian behaviour is assumed then these could be derived from predicted water uptake graphs. The concentration at one face could be set to saturation and a reflective boundary condition applied to the opposite face. The diffusivity in the direction perpendicular to those faces could then be calculated from the saturation and initial gradient of the graph using the inverse of equation (2). This was found to be inappropriate for two reasons:

a) By default a reflective boundary condition was also applied to the faces orthogonal to the diffusion direction, i.e. zero flow was imposed through these faces. This is not necessarily the case, for example it does not apply to diffusion at 0° through a 45° layer of a laminate.
b) Because the sample was non-homogeneous, the initial gradient of the water uptake graph could be non-linear and did not in general represent the overall behaviour of the structure.

Point (a) was resolved firstly by forcing the structure and finite element mesh to represent a repeating unit cell, i.e. the geometry and nodes of each face were identical to those on the opposite face. The cells did not have to be symmetric internally. Then, for example for diffusion in the z direction, boundary conditions were applied to mimic a plate which was infinite in the x and y directions. The relative concentration at each node on the minimum "x" face was forced to be equal to that at the node directly opposite on the maximum "x" face, and similarly for the "y" faces. For diffusion in other directions equivalent conditions were applied.

For point (b), the reflective boundary condition which produced a water uptake curve leading to saturation was replaced by one which gave steady state diffusion through the sample. For example, for diffusion in the z direction, the minimum "z" face was fixed at saturation, and the maximum "z" face at zero. At steady state, applying Fick's first law to the sample as a whole and to individual elements, an effective diffusivity D_{eff} was calculated from

$$D_{eff} = \left(\frac{h}{M_\infty}\right) \langle [P] \{\nabla C^*\}.\{n\} \rangle \quad (5)$$

where h is the sample thickness in the diffusion direction, M_∞ is the overall saturation concentration of the sample, {n} is the vector in the diffusion direction, and ‹› signifies a volume average. This averages the flux over all elements and so takes account of inhomogeneity in the sample.

3.4. Modelling procedure

Finite element (FE) modelling at each scale consisted of three activities:

1) A composite structure was created using the textile generation package Texgen [10].
2) A tetrahedral mesh was produced for this structure using Altair Hypermesh [11]. Tetrahedral elements were chosen because these can more accurately represent the geometry between closely packed fibres and yarns.
3) FE calculations were carried out using in-house Fortran software based on the methods described in Smith and Griffiths [12].

3.5. Predicted effect of fibre volume fraction and fibre distribution

A number of different unit cells were created at individual fibre scale to investigate the effect of fibre volume fraction and fibre distribution on the predicted diffusivity orthogonal to the fibres. These included uniform square and hexagonal arrangements, and random distributions, with varying but non-zero spacing and in each case with a range of fibre volume fractions. The resin diffusivity was set to $100x10^{-14}$ m^2/sec. As can be seen from figure 3(a), the diffusivity clearly reduced with increasing fibre volume fraction, as expected. For a particular V_f, the fibre distribution led to a variation of up to 15% of the resin diffusivity. However even at high V_f the predicted values were no less than 40% of D_r. Whilst small gaps between fibres clearly reduced the diffusivity to some extent, only the increase in diffusion path lengths caused by touching fibres led to predicted diffusivities in the range measured. In agreement with other studies, this corresponded to random arrangements of fibres, an example of which is shown in figure 3(b).

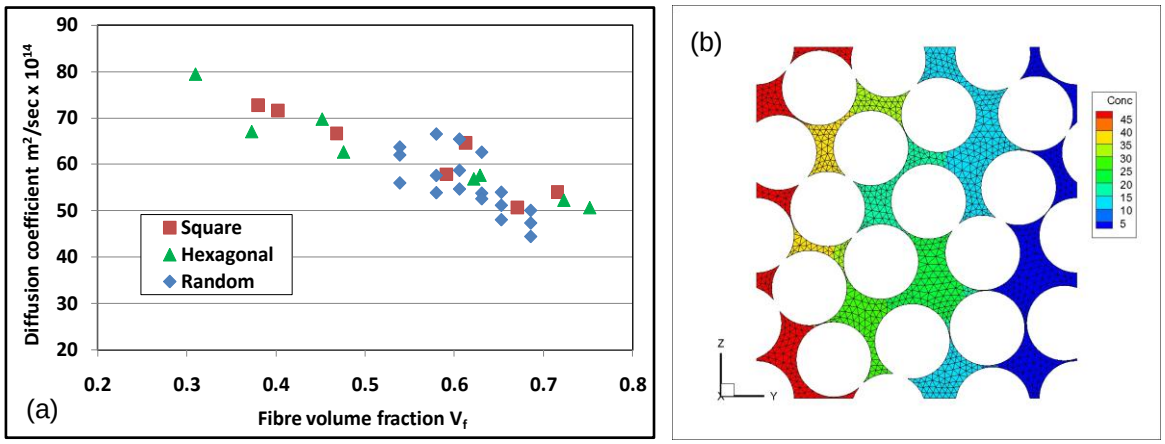

Figure 3. (a) Variation of diffusivity orthogonal to fibres in fibre rich region with fibre volume fraction **a**nd distribution (b) Example of random fibre arrangement used for unit cell in fibre-rich region, with concentration profile (kg/m^3) for y-direction diffusion at steady state

3.6. Extension of model capabilities to larger scale

Although the results above were for a unidirectional composite, the model allows for full directionality, so that for each element the primary axes of the composite (along, across and through the fibres) can be at any orientation in relation to the sample as a whole. This enables structures such as multi-layer laminates and weaves to be simulated. Modelling at this scale is being developed with an example of partial saturation of a weave structure shown in figure 4(b). In addition the long term effects shown in figure 2 will be incorporated into the model.

4 Model validation

Table 2 shows the predicted diffusivities at the two scales of modelling carried out. The value $D_{yz1,pred}$ was obtained from a unit cell with individual fibres representative of the fibre-rich regions of the composite, with a typical V_f of 0.75. This is shown in figure 3(b) with colours indicating the concentration profile at steady state when diffusion was in the y-direction. Fibre-rich yarns, with $D_x = D_r$, $D_y = D_z = D_{yz1,pred}$ were then embedded in resin in a structure representative of the whole composite, as shown in figure 4(a). This also shows the concentration profile for diffusion in the z-direction at steady state. Diffusivities $D_{y2,pred}$ and $D_{z2,pred}$ were calculated. For the Fickian diffusion modelled, the predicted ratios D_y/D_r and D_z/D_r were determined by the unit cell geometries so were the same for all conditions. The graph in table 2 compares these with the measured values. It can be seen that a close match to the average was achieved.

		Fibre rich unit cell	UD composite	
Condition	D_r	$D_{yz1,pred}$	$D_{y2,pred}$	$D_{z2,pred}$
	Diffusivities in $m^2/sec \times 10^{14}$			
23°C in water	12.1	1.85	5.33	1.93
40°C in water	32.0	4.90	14.1	5.11
70°C in water	141	21.7	62.5	22.6
70°C, 45% RH	186	28.6	82.3	29.9
70°C, 60% RH	185	28.3	81.5	29.5
70°C, 85% RH	159	24.4	70.3	25.5

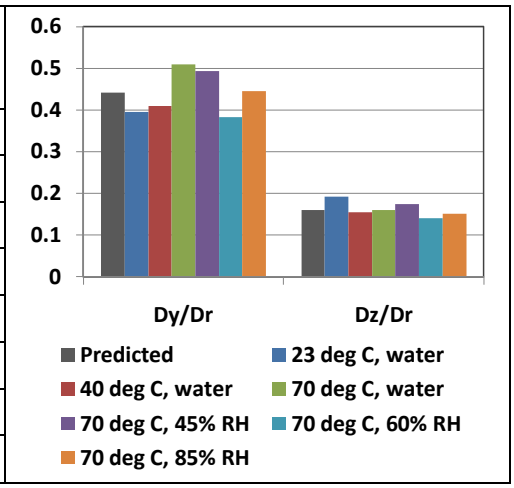

Table 2. Predicted diffusivities for fibre rich unit cell and UD composite. The graph shows a comparison of predicted ratios D_y/D_r and D_z/D_r with measured values for the composite.

5 Conclusions

A multi-scale modelling mechanism has been developed which enables the results of simulations at the microstructural scale to be used to predict the diffusivities for a unidirectional composite. Overall diffusivities for a non-homogeneous structure in a single direction were predicted by modelling steady state diffusion through a semi-infinite plate. Data from water uptake trials of UD composite samples were used to derive diffusivities in all three directions, and comparison of these with predicted values showed that good agreement could be achieved. Accurate representation of the detailed microstructure, including both fibre volume fraction and fibre distribution, was found to be critical to matching the measured data. Modelling has been extended to cover multidirectional laminates and weaves but has yet to be validated.

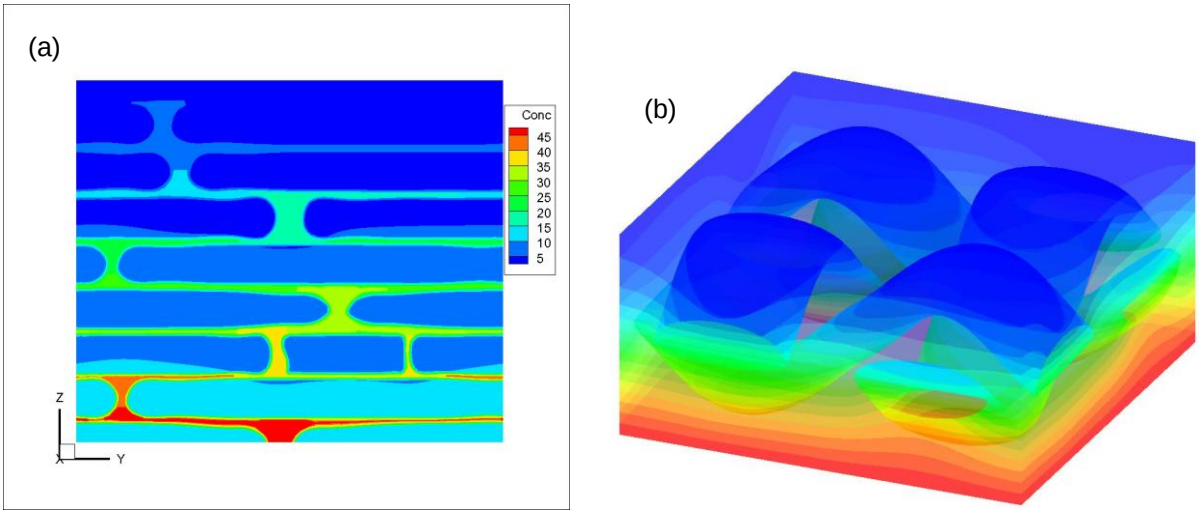

Figure 4. (a) Yarn / resin arrangement representing overall UD composite structure, with concentration profile (kg/m^3) for z-direction diffusion at steady state (b) Moisture profile in a partially saturated weave structure.

References

[1] Choi H.S., Ahn K.J., Nam J.D., Chun H.J. Hygroscopic aspects of epoxy/carbon fibre composite laminates in aircraft environments. *Composites*, **32A**, pp. 709-720 (2001).

[2] Arao Y., Koyanagi J., Hatta H., Kawada H. Analysis of Time-Dependent Deformation of CFRP Considering the Anisotropy of Moisture Diffusion. *Advanced Composite Materials*, **17**, pp. 359–372 (2008).

[3] Starink. M.J., Starink. L.M.P., Chambers. A. R. Moisture uptake in monolithic and composite materials: edge correction for rectanguloid samples. *J. Mater. Sci*, **37**, pp. 287-294 (2002).

[4] Aoki Y., Yamada K., Ishikawa T. Effect of hygrothermal condition on compression after impact strength of CFRP laminates. *Composites Science and Technology*, **68**, pp. 1376–1383 (2008).

[5] Kondo K., Taki T. Moisture Diffusivity of Unidirectional Composites. *Journal of Composite Materials*, **16**, pp. 82-93 (1982).

[6] Vaddadi P., Nakamura T., Singh R.P. Inverse analysis for transient moisture diffusion through fiber-reinforced composites. *Acta Materialia*, **51** pp. 177–193 (2003).

[7] Tang X., Whitcomb J.D., Li Y., Sue H.-J. Micromechanics modelling of moisture diffusion in woven composites. *Composites Science and Technology*, **65/6**, pp. 817–826 (2005).

[8] Laurenzi S., Albrizio T., Marchetti M. Modelling of Moisture Diffusion in Carbon Braided Composites. *International Journal of Aerospace Engineering*, **2008**, Article id 294681 (2008).

[9] Arnold J., Korkees F., Alston S. *The Long-Term Water Absorption and Desorption Behaviour of Carbon-fibre / Epoxy Composites* in "Proceeding of *15th European Conference on Composite Materials"*, Venice, Italy, (2012).

[10] Texgen open source software. Developed by University of Nottingham, UK. http://texgen.sourceforge.net/index.php/Main_Page.

[11] Altair Hypermesh. Altair Engineering Inc., Troy, Mich. http://www.altairhyperworks.com.

[12] Smith I.M., Griffiths D.V. *Programming the Finite Element Method, 3rd Edition*. John Wiley & Sons, Chichester (1998).